

Photon Sorting, Efficient Bell Measurements, and a Deterministic Controlled-Z Gate Using a Passive Two-Level Nonlinearity

T. C. Ralph,¹ I. Söllner,² S. Mahmoodian,² A. G. White,¹ and P. Lodahl²

¹Centre for Quantum Computation and Communication Technology, School of Mathematics and Physics, University of Queensland, Brisbane, Queensland 4072, Australia

²Niels Bohr Institute, University of Copenhagen, Blegdamsvej 17, DK-2100 Copenhagen, Denmark

(Received 11 February 2015; published 30 April 2015)

Although the strengths of optical nonlinearities available experimentally have been rapidly increasing in recent years, significant challenges remain to using such nonlinearities to produce useful quantum devices such as efficient optical Bell state analyzers or universal quantum optical gates. Here we describe a new approach that avoids the current limitations by combining strong nonlinearities with active Gaussian operations in efficient protocols for Bell state analyzers and controlled-SIGN gates.

DOI: 10.1103/PhysRevLett.114.173603

PACS numbers: 42.50.Ex, 03.67.Ac, 03.67.Lx, 42.50.Dv

Introduction.—It has long been the dream of the quantum optics community to use nonlinear optical interactions to produce deterministic quantum logic operations, such as a controlled-SIGN (CZ) gate, between individual photons [1]. In combination with easily implemented single qubit operations, the CZ gate produces a universal set of quantum logic operations that would enable applications from quantum repeaters to full scale quantum computation with photons. Unfortunately, not only is it very difficult to achieve the strengths of nonlinearity required for such gates, but it has been predicted for several candidate systems that strong nonlinearities inevitably add noise and/or distort the optical modes of the single photons sufficiently that successful operation, even under ideal conditions, is impossible [2–4].

One such candidate system with various possible physical implementations is a single two-level emitter deterministically coupled to a one-dimensional photonic waveguide. We will refer to such a system here as a two-level scatterer (TLS). One interesting capability of such systems is to separate the single- and two-photon components of an optical mode into two separate modes. This has been referred to as photon sorting [5]. In principle, photon sorting, if efficient and mode preserving, could be used to perform full Bell measurements and to implement deterministic quantum logic gates between photonic qubits. However, it has been shown that the TLS introduces mode distortion between the single- and two-photon components in the form of spectral entanglement of the two-photon component [3], which has been argued to be unavoidable [4]. As a result, photon sorting is inefficient. While it has been shown that by combining multiple interactions with a TLS with linear optics it is possible to perform near deterministic Bell measurements, the proposed scheme requires 80 separate scattering events to obtain a probability of success of about 95% [5].

Here we show that by adding active Gaussian optics to our tool box of scatterer plus passive linear optics we are able to perform a deterministic Bell measurement using only 4 interactions with a TLS. Similarly, in principle, it becomes possible to implement deterministic quantum logic gates in this way. Ironically, it is by exploiting the inherent mode distortion of the scatterer that these operations become possible.

Action of the scatterer.—We consider a TLS formed by placing a two-level emitter in a nanophotonic cavity or waveguide that is designed for unidirectional interaction [6–8], cf. Fig. 1(a). The monochromatic creation operator for the input mode, with wave number k , is scattered such that the corresponding creation operator for the output mode is given by [9]

$$\hat{a}_{k,\text{in}}^\dagger \rightarrow t_k \hat{a}_{k,\text{out}}^\dagger, \quad (1)$$

where

$$t_k = \frac{ck - \omega_0 + i(\gamma - \Gamma)/2}{ck - \omega_0 + i(\gamma + \Gamma)/2}, \quad (2)$$

with c the speed of light, ω_0 the resonant frequency of the two-level emitter, Γ the coupling strength between the emitter and a unidirectional waveguide mode and γ , the coupling strength of the emitter to modes other than the directional waveguide mode of interest. Equation (1) describes a linear transformation similar to that produced by reflection from a single ended optical cavity. In general, the output state will be mixed due to losses into other modes and the relevant figure of merit is the directional β factor defined as $\beta_{\text{dir}} = \Gamma/(\gamma + \Gamma)$ [8]. In the ideal case for which losses are negligible, i.e., $\gamma = 0$, the scattering is unitary and we can write the input-output relation for a single-photon state with an arbitrary pulse shape $f(k)$ as

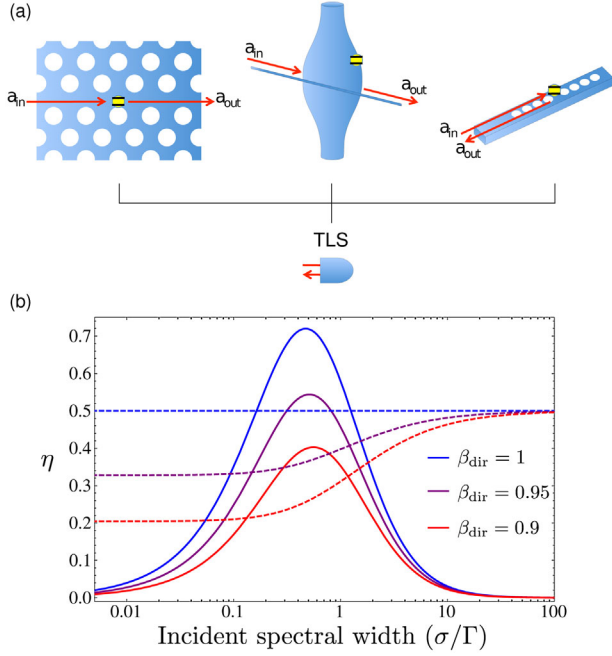


FIG. 1 (color online). (a) Possible physical implementations of an efficient TLS exploiting unidirectional coupling obtained by implementing a two-level emitter in a chiral photonic-crystal waveguide (left) [8], a whispering-gallery resonator (middle) [7], or a photonic-crystal cavity (right) [6]. (b) η as a function of the spectral width of the incoming pulse in the case of a Lorentzian spectral response and for three different values of the β_{dir} factor ($\beta_{\text{dir}} = 1$ is the top solid line). The dashed lines show $\epsilon_1^2/2$ for the different values of β_{dir} . Where the solid and corresponding dashed lines meet are the optimal operation points. In order to minimize loss, the crossing points at higher spectral widths should be chosen as the operation points.

$$\begin{aligned}
 |1_f\rangle &= \int dk f(k) \hat{a}_{k,\text{in}}^\dagger |0\rangle \\
 \rightarrow |1_{f'}\rangle &= \int dk f(k) t_k \hat{a}_{k,\text{out}}^\dagger |0\rangle.
 \end{aligned} \quad (3)$$

We now consider two-photon inputs. The equivalent of Eq. (1) for a pair of monochromatic creation operators with wave numbers k_1 and k_2 is [3,10]

$$\begin{aligned}
 \hat{a}_{k_1,\text{in}}^\dagger \hat{a}_{k_2,\text{in}}^\dagger &\rightarrow t_{k_1} \hat{a}_{k_1,\text{out}}^\dagger t_{k_2} \hat{a}_{k_2,\text{out}}^\dagger \\
 &+ T_{k_1,k_2,p_1,p_2} \hat{a}_{p_1,\text{out}}^\dagger \hat{a}_{p_2,\text{out}}^\dagger,
 \end{aligned} \quad (4)$$

where

$$T_{k_1,k_2,p_1,p_2} = \frac{i\sqrt{\Gamma}}{2\pi} \delta(k_1 + k_2 - p_1 - p_2) s_{p_1} s_{p_2} (s_{k_1} + s_{k_2}), \quad (5)$$

with $s_k = (1/i\sqrt{\Gamma})(1 - t_k)$. Equation (4) describes a highly nonlinear interaction that produces entanglement between the spectral components of the two input photons. Again considering the ideal case for which $\gamma = 0$, we can write

$$|2_f\rangle \rightarrow |2_{f'}\rangle + |2_{fb}\rangle, \quad (6)$$

where

$$|2_{f'}\rangle = \int dk_1 dk_2 f(k_1) t_{k_1} \hat{a}_{k_1,\text{out}}^\dagger f(k_2) t_{k_2} \hat{a}_{k_2,\text{out}}^\dagger |0\rangle \quad (7)$$

and

$$\begin{aligned}
 |2_{fb}\rangle &= \int dk_1 dk_2 dp_1 dp_2 T_{k_1,k_2,p_1,p_2} \\
 &\times f(k_1) \hat{a}_{p_1,\text{out}}^\dagger f(k_2) \hat{a}_{p_2,\text{out}}^\dagger |0\rangle.
 \end{aligned} \quad (8)$$

The solution in the form of Eq. (6) was presented in Ref. [5]. However, it is clear from the normalization of Eq. (6) that the states of Eq. (7) and Eq. (8) are not orthogonal. Improved physical insight into the process can be obtained by rewriting Eq. (6) in terms of orthogonal states. We obtain

$$|2_f\rangle \rightarrow (1 - 2\eta)|2_{f'}\rangle + 2\sqrt{\eta(1 - \eta)}|\bar{2}_{f'}\rangle, \quad (9)$$

where

$$\eta = \frac{1}{2} |\langle 2_{f'} | 2_{fb} \rangle|, \quad (10)$$

and $|\bar{2}_{f'}\rangle$ is a normalized state satisfying $\langle 2_{f'} | \bar{2}_{f'} \rangle = 0$. The value of η depends on the specific pulse shape chosen for the input state. It can be calculated analytically for pulses with a Lorentzian spectral shape and is found to be

$$\eta = \frac{4\Gamma^2\sigma(3\Gamma^2 + 38\Gamma\sigma + 96\sigma^2)}{(\Gamma + 2\sigma)^3(3\Gamma + 2\sigma)(\Gamma + 6\sigma)}, \quad (11)$$

where σ is the width of the Lorentzian. A plot of the behavior of Eq. (11) as a function of σ is shown in Fig. 1(b). If it was possible to achieve $\eta = 1$ then one could directly use two TLSs to build a deterministic CZ gate as the transformation would essentially be a nonlinear SIGN shift (NS) gate—imposing a phase flip on the two-photon component but not the single-photon component of the state [11]. It would also be possible to achieve deterministic photon sorting via the scheme in Ref. [5]. Unfortunately, numerically it appears that η is bounded by $0 \leq \eta < 0.75$.

Efficient photon sorting.—One solution to this problem is to operate instead with $\eta = 0.5$, which is easily achieved with either a Lorentzian [see Fig. 1(b)] or Gaussian [5] mode function. An arbitrary superposition of single and two-photon components is then transformed by the TLS as

$$\alpha|1_f\rangle + \xi|2_f\rangle \rightarrow \alpha|1_{f'}\rangle + \xi|\bar{2}_{f'}\rangle. \quad (12)$$

With this choice of parameters the one- and two-photon components are completely mapped into copropagating,

but orthogonal, spatiotemporal modes which can, in principle, be perfectly separated with Gaussian transformations. This conclusion continues to be true for $\beta_{\text{dir}} < 1$ as shown in Fig. 1(b). Now the matching condition is $\eta = \epsilon_1^2/2$, where ϵ_1 is the probability that a single photon is scattered into the output mode by the TLS (see Supplemental Material [12] for details).

Because the modes have overlapping spectral and temporal domains, passive filtering will not be sufficient to perfectly separate them—instead active filtering is required. In particular, consider sum frequency generation (SFG). It was shown in Ref. [13] that by using suitably engineered SFG a quantum pulse gate can be produced that can efficiently extract a particular spatiotemporal mode from a multimode field. This works by choosing the pump field to perfectly match the spatiotemporal mode to be extracted. After interaction with a $\chi^{(2)}$ nonlinear crystal it is this—and only this—mode that is converted to the sum frequency. A passive frequency filter will then suffice to split the field into separate beams. The procedure is shown diagrammatically in Fig. 2(a) and can be represented mathematically as

$$\begin{aligned} (\alpha|1_{f'}\rangle + \xi|2_{f'}\rangle)|0\rangle_a &\xrightarrow{\text{TLS}} (\alpha|1_{f'}\rangle + \xi|\bar{2}_{f'}\rangle)|0\rangle_a \\ &\xrightarrow{\text{SFG}} \alpha|0\rangle|1_{f'}\rangle_a + \xi|\bar{2}_{f'}\rangle|0\rangle_a, \end{aligned} \quad (13)$$

where the mode function of the classical pump beam for the SFG is $t_k f(k)$ and the ket (initially in the vacuum state)

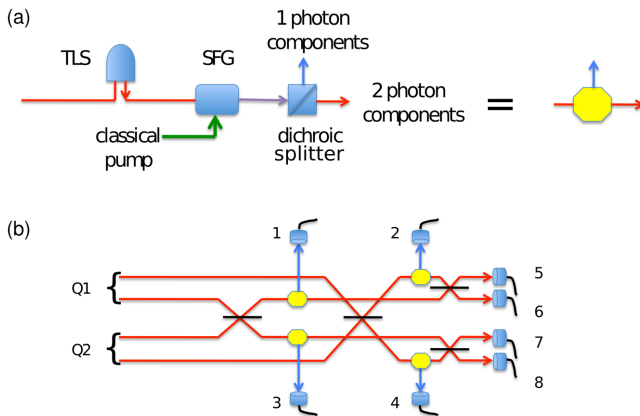


FIG. 2 (color online). Components of the photon sorter and Bell measurement device. (a) The photon sorter is constructed from a TLS followed by SFG, where the classical pump is in the mode f' , followed by a dichroic beam splitter that separates the single-photon component at the sum frequency from the two-photon component at the original frequency. (b) A Bell measurement can be implemented with linear optics and four-photon sorters as shown. The four Bell states are unambiguously determined by the measurement of photons at particular detector combinations. In particular, $|\psi^+\rangle$: 1, 4, or 3, 2; $|\psi^-\rangle$: 1, 2 or 3, 4; $|\phi^+\rangle$: 5, 8 or 6, 7; $|\phi^-\rangle$: 5, 7 or 6, 8.

labeled with the subscript a is an ancilla mode at the sum frequency. Hence, using a single TLS plus sum frequency generation and passive filtering it is possible to produce a deterministic photon sorter. One should compare this with Ref. [5] where (assisted by only linear optics) 10 TLSs (or perhaps 10 interactions with a single TLS) are required to achieve, in principle, 95% separation of the one and two-photon components.

Bell measurement.—Equipped with a deterministic photon sorter it is straightforward to construct a circuit from passive linear optics that can implement deterministic Bell measurements on dual rail single-photon qubits. A dual rail qubit is where the logical value of the qubit is determined by which of the two orthogonal modes is occupied, i.e., $|0\rangle_L = |1\rangle_u|0\rangle_l$ and $|1\rangle_L = |0\rangle_u|1\rangle_l$, where number kets for the two modes are labeled u (upper) and l (lower). The circuit is shown in Fig. 2(b), where the qubits are labeled as Q1 and Q2 at the inputs and the orthogonal modes making up the qubits are shown as separate spatial rails. We note that it does not matter that the single-photon and two-photon components of the state end up in different spatiotemporal modes (at different average frequencies) because (i) the coherent interactions that occur after the photon sorters only superpose modes containing two-photon components, hence, these interactions occur between matched modes; and (ii), in the end destructive measurements are made on all the modes that have been through the photon sorters. If $\beta_{\text{dir}} < 1$ then there will be loss in the TLS and there will be heralded failure events when the photons do not make it through the circuit (see Supplemental Material [12] for a discussion and graph of the probability of success).

Deterministic CZ gate.—Given deterministic Bell measurements it is possible to construct a deterministic CZ gate using the techniques of gate teleportation [14] and linear optical quantum computing [11]. The necessary circuit is, however, quite complex, requiring significant off-line optical resources for state preparation and, hence, either quantum memory or sophisticated real-time optical switching. In addition, such a gate necessarily includes electro-optic feedforward.

It is interesting to ask if, alternatively, the TLS nonlinearity plus Gaussian optics is sufficient to directly implement a deterministic CZ gate in an all-optical arrangement. In the following, we show that this is possible, in principle, with TLS, SFG, gradient echo memory (GEM) and linear optics. The setup is shown schematically in Fig. 3. We start with an input light field containing zero-, one-, and two-photon terms that can be written as

$$\alpha|0\rangle + \xi|1_{f'}\rangle + \gamma|2_{f'}\rangle. \quad (14)$$

As described in the previous section, the combination of TLS and SFG with a suitable classical pump leads to a state of the form

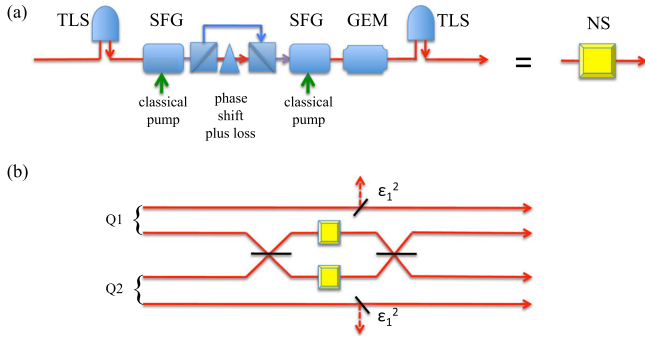


FIG. 3 (color online). Components of the NS gate and deterministic CZ gate. (a) The NS gate is constructed from a TLS followed by SFG, where the classical pump is in the mode f' . This is followed by a π phase shift which is imposed only on the two-photon term. If $\beta_{\text{dir}} < 1$ then the loss is also applied only to the two-photon term. A second SFG then reverses the frequency shift, followed by short term storage in a GEM that inverts the pulse shape. Finally, the inverted pulse is sent through a second TLS that recombines the one- and two-photon terms back into the same mode. If the initial mode shape was time symmetric then the overall effect will be that of an NS gate, i.e., to impose a π phase shift only on the two-photon terms while leaving the mode shapes unchanged. (b) The resultant NS gates can be incorporated in a simple linear optical circuit to produce a CZ gate. Beam splitters on the outer arms are required if $\beta_{\text{dir}} < 1$ in order to resymmetrize the state.

$$\alpha|0\rangle|0\rangle_a + \xi|0\rangle|1_{f'}\rangle_a + \gamma|\bar{2}_{f'}\rangle|0\rangle_a. \quad (15)$$

Because of the different frequencies of the one- and two-photon components they can be addressed individually, hence, we impose a π phase shift only on the two-photon term—in Fig. 3 we represent this by spatially separating the beams, imposing the phase shift, and then recombining them, but in practice easier techniques, such as using a wave shaper may be available. SFG is a reversible process, thus, by choosing a suitable phase relationship between the classical pump and the beams, the one-photon component can be converted back to its original centre frequency. The output state after this manipulation is

$$\alpha|0\rangle + \xi|1_{f'}\rangle - \gamma|\bar{2}_{f'}\rangle. \quad (16)$$

We now wish to undo the initial separation of the one and two-photon terms into orthogonal modes by interacting with the TLS a second time. However, the mode distortion is not time symmetric so we must first invert the pulse shape of the modes. This can be achieved using a gradient echo memory [15,16]. The GEM can be thought of as a material containing an ensemble of two-level atoms that can absorb and store an incident light pulse as it passes through it. During the storage or writing process a field gradient is applied to the material, producing a spatially selective storage of the different frequency components of the input signal. To release or readout the pulse, the gradient is

reversed and the light emerges from the other end of the material. However, the reversal of the gradient results in the shape of the pulse being inverted between input and output. In particular, in the limit that the storage bandwidth of the memory is much larger than the bandwidth of the pulse and the storage time of the memory is much longer than the pulse length, the action of the memory on an optical mode operator can be expressed as [17]

$$\hat{a}_{\text{in}}(t) = \int dk F(k) e^{-ikt} \hat{a}_k \\ \xrightarrow{\text{GEM}} \int dk F(-k) e^{-ik(t-T)} \hat{a}_k. \quad (17)$$

The pulse is delayed by a time T and the pulse shape is inverted. An explicit calculation confirms that if the state of Eq. (16) is transformed according to Eq. (17) and then interacted a second time with a TLS, the final output is

$$\alpha|0\rangle + \xi|1_{f'}\rangle - \gamma|2_{f'}\rangle, \quad (18)$$

where we have assumed the initial mode shape was time symmetric. The total transformation from Eqs. (14) to (18) is characteristic of a nonlinear-SIGN (NS) gate, as introduced in Ref. [11]. Two NS gates can be combined with linear optics to make a CZ gate as shown in Fig. 3(b). Consider first the case for which $\beta_{\text{dir}} = 1$ and, hence, $\epsilon_1 = 1$. All but one of the possible two qubit logical input states lead to only zero-or one-photon occupation of the interferometer containing the NS gates in the central region of the circuit. The exception is the logical state with the lower rail of Q1 occupied and the upper rail of Q2 occupied. In this case, because of the Hong Ou Mandel effect [18], the *only* allowed photon arrangements in the central interferometer are a pair of photons through the upper NS gate or a pair of photons through the lower NS gate. Hence, only in this case a phase is imposed on the output state as required for a CZ gate. Notice that all the mode distortions are undone, hence a network of such gates may be used to implement universal quantum computation using single-photon inputs. In Ref. [11] the NS gate was implemented with linear optics and had a probability of success of 25%, hence leading to a CZ gate with probability of success 6.25%. Here the NS gate and hence the CZ gate are, in principle, deterministic. In the case for which $\beta_{\text{dir}} < 1$ the gate will no longer be deterministic because photons can be lost in the TLS. In this case additional loss elements need to be introduced into the gate to ensure the qubit states do not become skewed [see Fig. 3(b) and the Supplemental Material [12] for discussion and plot of the probability of success].

Discussion.—We have shown that a deterministic Bell measurement and CZ gate can be implemented by combining a nonlinear element with active and passive Gaussian optics. This is possible in spite of (or perhaps because of) the mode distortion produced by the nonlinear element. We

now discuss the challenges involved in implementing our schemes by briefly reviewing the state of the art for the various components.

Different platforms have been experimentally shown to be suitable for constructing a TLS [19] [see Fig. 1(a)]. Single atoms and single quantum dots that are coupled to either photonic nanostructures [6,20–22] or whispering gallery mode resonators [7,23] are the most promising at optical frequencies. Furthermore, transmon qubits in 1D transmission lines can be employed in the microwave regime [24]. In the case of quantum dots in photonic-crystal waveguides, coupling efficiencies of 98.4% have been demonstrated in experiments on emission dynamics [22]. For the coherent scattering applications considered here any pure dephasing, spectral diffusion, and Raman scattering into the phonon-sideband will limit the performance. Excitingly, 97% indistinguishability of single photons [25] and about 95% of the emission in the zero-phonon line [26] have been experimentally reported. Mode selectivity of 80%, with bandwidths compatible with quantum dot TLSs, has been experimentally demonstrated for SFG [27], with excellent prospects for improvement. Hence, the technology required for implementing the Bell measurement protocol currently exists. The bottle neck in our CZ gate protocol is likely to be the GEM memories which, while showing good storage times and efficiency, currently operate with bandwidths around a MHz—and, hence, are currently incompatible with quantum dot bandwidths of around 320 MHz. Nevertheless, there does not seem to be any, in principle, reasons why GEM of the necessary bandwidth could not be realized.

TCR acknowledges useful discussions with Christine Silberhorn, Ben Buchler and Andre Carvalho. This research was supported by the Australian Research Council (ARC) under the Centre of Excellence for Quantum Computation and Communication Technology (CE110001027). I. S., S. M., and P. L. gratefully acknowledge financial support from the Danish Council for Independent Research (Natural Sciences and Technology and Production Sciences) and the European Research Council (ERC consolidator Grant ALLQUANTUM).

-
- [1] G. J. Milburn, *Phys. Rev. Lett.* **62**, 2124 (1989).
 - [2] J. H. Shapiro, *Phys. Rev. A*, **73**, 062305 (2006).
 - [3] J.-T. Shen and S. Fan, *Phys. Rev. Lett.* **98**, 153003 (2007).
 - [4] S. Xu, E. Rephaeli, and S. Fan, *Phys. Rev. Lett.* **111**, 223602 (2013).
 - [5] D. Witthaut, M. D. Lukin, and A. S. Sørensen, *Europhys. Lett.* **97**, 50007 (2012).
 - [6] T. G. Tiecke, J. D. Thompson, N. P. deLeon, L. R. Liu, V. Vuletić, and M. D. Lukin, *Nature (London)* **508**, 241 (2014).

- [7] J. Volz, M. Scheucher, C. Junge, and A. Rauschenbeutel, *Nat. Photonics* **8**, 965 (2014).
- [8] I. Söllner, S. Mahmoodian, S. Lindskov Hansen, L. Midolo, A. Javadi, G. Kirsanske, T. Pregnolato, H. El-Ella, E. H. Lee, J. D. Song, S. Stobbe, and P. Lodahl, arXiv:1406.4295.
- [9] J.-T. Shen and S. Fan, *Opt. Lett.* **30**, 2001 (2005).
- [10] J.-T. Shen and S. Fan, *Phys. Rev. A* **76**, 062709 (2007).
- [11] E. Knill, R. Laflamme, and G. J. Milburn, *Nature (London)* **409**, 46 (2001).
- [12] See Supplemental Material at <http://link.aps.org/supplemental/10.1103/PhysRevLett.114.173603> for details of theory when loss is present in the TLS and plots of probability of success under these conditions.
- [13] A. Eckstein, B. Brecht, and C. Silberhorn, *Opt. Express* **19**, 13770 (2011).
- [14] D. Gottesman and I. L. Chuang, *Nature (London)* **402**, 390 (1999).
- [15] A. L. Alexander, J. J. Longdell, M. J. Sellars, and N. B. Manson, *Phys. Rev. Lett.* **96**, 043602 (2006); G. Hétet, J. J. Longdell, A. L. Alexander, P. K. Lam, and M. J. Sellars, *Phys. Rev. Lett.* **100**, 023601 (2008).
- [16] M. P. Hedges, J. J. Longdell, Y. Li, and M. J. Sellars, *Nature (London)* **465**, 1052 (2010); M. Hosseini, B. M. Sparkes, G. Campbell, P. K. Lam, and B. C. Buchler, *Nat. Commun.* **2**, 174 (2011).
- [17] M. R. Hush, A. R. R. Carvalho, M. Hedges, and M. R. James, *New J. Phys.* **15**, 085020 (2013).
- [18] C. K. Hong, Z. Y. Ou, and L. Mandel, *Phys. Rev. Lett.* **59**, 2044 (1987).
- [19] P. Lodahl, S. Mahmoodian, and S. Stobbe, arXiv:1312.1079 [Rev. Mod. Phys. (to be published)].
- [20] A. K. Nowak, S. L. Portalupi, V. Giesz, O. Gazzano, C. DalSavio, P.-F. Braun, K. Karrai, C. Arnold, L. Lanco, I. Sagnes, A. Lemaître, and P. Senellart, *Nat. Commun.* **5**, 3240 (2014).
- [21] A. Goban, C.-L. Hung, S.-P. Yu, J. D. Hood, J. A. Muniz, J. H. Lee, M. J. Martin, A. C. McClung, K. S. Choi, D. E. Chang, O. Painter, and H. J. Kimble, *Nat. Commun.* **5**, 3808 (2014).
- [22] M. Arcari, I. Söllner, A. Javadi, S. Lindskov Hansen, S. Mahmoodian, J. Liu, H. Thyrrestrup, E. H. Lee, J. D. Song, S. Stobbe, and P. Lodahl, *Phys. Rev. Lett.* **113**, 093603 (2014).
- [23] K. Srinivasan and O. Painter, *Nature (London)* **450**, 862 (2007).
- [24] I.-C. Hoi, T. Palomaki, J. Lindkvist, G. Johansson, P. Delsing, and C. M. Wilson, *Phys. Rev. Lett.* **108**, 263601 (2012).
- [25] Y.-M. He, Y. He, Y.-J. Wei, D. Wu, M. Atataure, C. Schneider, S. Hofling, M. Kamp, C.-Y. Lu, and J.-W. Pan, *Nat. Nanotechnol.* **8**, 213 (2013).
- [26] K. Konthasinghe, J. Walker, M. Peiris, C. K. Shih, Y. Yu, M. F. Li, J. F. He, L. J. Wang, H. Q. Ni, Z. C. Niu, and A. Muller, *Phys. Rev. B* **85**, 235315 (2012).
- [27] B. Brecht, A. Eckstein, R. Ricken, V. Quiring, H. Suche, L. Sansoni, and C. Silberhorn, *Phys. Rev. A* **90**, 030302(R) (2014).